

Article

Mechanical Response of Cu/Sn58Bi-xNi/Cu Micro Solder Joint with High Temperatures

Xiangxia Kong^{1,2,*} , Junjun Zhai^{3,*}, Ruipeng Ma^{1,2}, Fenglian Sun⁴ and Xuemei Li⁵

¹ Department of Material Engineering, North China Institute of Aerospace Engineering, Langfang 065000, China; maruipeng202301@163.com

² Hebei Provincial Key Laboratory of Thermal Protection Materials, Langfang 065000, China

³ Department of Aeronautics and Astronautics, North China Institute of Aerospace Engineering, Langfang 065000, China

⁴ Department of Materials Science and Chemical Engineering, Harbin University of Science and Technology, Harbin 150040, China; sunfengl@hrbust.edu.cn

⁵ Department of Mechanical and Electronic Engineering, Qiqihar University, Qiqihar 161006, China; 02867@qqhru.edu.cn

* Correspondence: kongxx@nciae.edu.cn (X.K.); junzhai726@nciae.edu.cn (J.Z.)

Abstract: Sn58Bi solder is considered a promising lead-free solder that meets the performance requirements, with the advantages of good wettability and low cost. However, the low melting point characteristic of Sn58Bi poses a serious threat to the high-temperature reliability of electronic products. In this study, Sn58Bi solder alloy based on nickel (Ni) functionalization was successfully synthesized, and the effect of a small amount of Ni on creep properties and hardness of Cu/Sn58Bi/Cu micro solder joints at different temperatures (25 °C, 50 °C, 75 °C, 100 °C) was investigated using a nanoindentation method. The results indicate that the nanoindentation depth of micro solder joints exhibits a non-monotonic trend with increasing Ni content at different temperatures, and the slope of the indentation stage curve decreases at 100 °C, showing that the micro solder joints undergo high levels of softening. According to the observation of indentation morphology, Ni doping can reduce the indentation area and accumulation around the indentation, especially at 75 °C and 100 °C. In addition, due to the severe creep phenomenon at 100 °C, the indentation hardness rapidly decreases. The indentation hardness values of micro solder joints of Cu/Sn58Bi/Cu, Cu/Sn58Bi-0.1Ni/Cu, and Cu/Sn58Bi-0.2Ni/Cu at 100 °C are 14.67 ± 2.00 MPa, 21.05 ± 2.00 MPa, and 20.13 ± 2.10 MPa, respectively. Nevertheless, under the same temperature test conditions, the addition of Ni elements can improve the high-temperature creep resistance and hardness of Cu/Sn58Bi/Cu micro solder joints.

Keywords: micro solder joint; nanoindentation; creep property; hardness; high temperature



Citation: Kong, X.; Zhai, J.; Ma, R.; Sun, F.; Li, X. Mechanical Response of Cu/Sn58Bi-xNi/Cu Micro Solder Joint with High Temperatures. *Crystals* **2024**, *14*, 269. <https://doi.org/10.3390/cryst14030269>

Academic Editor: Indrajit Charit

Received: 22 February 2024

Revised: 4 March 2024

Accepted: 7 March 2024

Published: 10 March 2024



Copyright: © 2024 by the authors. Licensee MDPI, Basel, Switzerland. This article is an open access article distributed under the terms and conditions of the Creative Commons Attribution (CC BY) license (<https://creativecommons.org/licenses/by/4.0/>).

1. Introduction

With the development of science and technology, the industry not only has higher requirements for the reliability of assembly and packaging, but also has requirements for the assembly temperature of products [1]. It is hoped that alloy solder with a liquidus temperature lower than 200 °C will be able to be used to complete the assembly under low-soldering-temperature conditions. Sn58Bi solder alloy has become a promising lead-free solder due to its many advantages, such as good wettability, low melting point, and low cost [2–4]. However, it is a matter of concern that SnBi eutectic solder has some disadvantages, like low ductility, poor drop resistance, and fatigue characteristics [5–8]. In addition, Sn58Bi solder also causes electro-migration and thermal migration during use [9,10].

To improve the performance of Sn58Bi lead-free solder, a large amount of research based on experimental approaches has been proposed; for example, nanoparticles, metal compounds, and trace elements were added to Sn58Bi lead-free solder [11–15]. Jeong et al. [16]

studied the effects of different Ag nanoparticle (Ag-NP) content on the interface reaction and mechanical properties of Sn58Bi solder joints. The addition of an appropriate amount of Ag-NPs inhibits the growth of the interfacial intermetallic compound (IMC) and reduces the brittle fracture of the interface. However, excessive addition of Ag-NPs will degrade the mechanical properties of the solder joints. Yang et al. [17] added CuZnAl particles with a mass fraction of 0~0.4 wt.% in Sn58Bi solder, and found that the addition of an appropriate amount of CuZnAl particles significantly improved the wettability of Sn58Bi solder. When adding 0.1~0.2 wt.% CuZnAl particles, the microstructure of Sn58Bi solder is significantly refined, and the growth of the interfacial intermetallic compound (IMC) can also be inhibited. Qsa et al. [2] studied the interfacial reaction and mechanical properties of Sn58Bi-xCr (x = 0, 0.1, 0.2, and 0.3 wt.%) solder joints. The research found that the microstructure of Sn58Bi composite solder joints was obviously refined with 0.2 wt.% Cr, and the tensile properties were better than other alloy components after isothermal aging treatment at 100 °C. Meanwhile, the average thickness of the IMC became thinner with the increase of Cr content.

The addition of Ni can significantly suppress the coarsening phenomenon of the microstructure and achieve the goal of improving the mechanical properties of solders [6,17–20]. Kanlayasiri et al. [21] studied the effect of Ni on the physical properties of Sn58Bi solder and the interfacial reaction between the solder with copper substrate. The research indicated that the addition of Ni can refine the microstructure of the solder and produce Ni₃Sn₄ compounds in the solder. When the content of Ni is 0.1 wt.%, the tensile strength of the solder can be improved. Yang et al. [22] found that during the solid-state aging process, Ni can reduce the coefficient of thermal expansion (CTE) and improve the microstructure of SnBi solder, leading to an increase in the elastic modulus, tensile strength, and yield strength of SnBi solder. Fleshman et al. [23] investigated the relationship between different Ni contents and shear properties before and after aging in Sn-1.2Ag-0.5Cu-xNi (SAC1205-xNi) (wt.%; x = 0, 0.05, 0.1)/OSP Cu solder joints. The results of the slow shear test showed that compared with SAC1205/OSP Cu solder joints, both SAC1205-0.05Ni/OSP Cu and SAC1205-0.1Ni/OSP Cu solder joints exhibited a 9% increase in peak force before aging. Compared with solder joints without Ni after aging, the peak forces of SAC1205-0.05Ni/OSP Cu and SAC1205-1Ni/OSP Cu solder joints were increased by 10% and 12%, respectively. They also pointed out that in advanced electronic packaging, solder joints with a small amount of Ni doping tend to exhibit better mechanical reliability before and after aging. Cao et al. [24] found that adding 0.05 wt.% Ni to the Sn2.5Ag0.7Cu0.1RE/Cu solder joints can inhibit the growth of IMC and reduce the roughness and average thickness of the interface IMC layer under the thermal cycling load. It was found that 0.05 wt.% Ni also can be improve the shear strength of the Sn2.5Ag0.7Cu0.1RE/Cu solder joints. In addition, Ni can significantly reduce the growth of Cu₃Sn during soldering and thermal aging [25].

Based on the achievement above, the addition of Ni elements has significantly improved the mechanical properties of Sn58Bi solder at room temperature, but few studies have paid attention to the influence of Ni content on the service performance of Cu/Sn58Bi/Cu micro solder joints at high temperatures. Due to the fact that high-temperature creep deformation and failure of micro solder joints can more effectively predict the strain trend and fracture life than high-temperature strength, studying the effect of trace Ni addition on the high-temperature service performance of Cu/Sn58Bi/Cu micro solder joints and improving the creep resistance of Cu/Sn58Bi/Cu micro solder joints are of great significance for improving the reliability of electronic products.

In this work, combining the low cost and excellent performance of Ni, the Sn58Bi-xNi (x = 0, 0.1, 0.2 wt.%) solders were firstly prepared by metal smelting. In order to fully understand the effect of Ni addition on the high-temperature mechanical behavior of Cu/Sn58Bi/Cu micro solder joints, Cu/Sn58Bi-xNi/Cu micro solder joints were prepared by classical reflow soldering method. Finally, based on the advantages of nanoindentation technology, which can minimize damage to the specimen and accurately evaluate the

mechanical properties of the microstructure, the high-temperature creep performance and hardness of Cu/Sn58Bi-xNi/Cu micro solder joints were studied. Furthermore, the indentation morphology of Cu/Sn58Bi-xNi/Cu micro solder joints at different temperatures was also observed and analyzed using the scanning electron microscopy (SEM) method, and some important conclusions were obtained. It is hoped that this effort can contribute to the further development of the microelectronic packaging field.

2. Materials and Methods

In this research, Sn58Bi-xNi solder was obtained by smelting pure metals Sn, Bi, and Ni with a purity of 99.99%, where x is 0, 0.1, and 0.2 wt.%. The melting temperatures of Sn58Bi-xNi solder alloys were measured by differential scanning calorimetry (DSC) under the condition that the heating rate and cooling rate were 10 °C/min and N₂ was introduced for protection [26]. The 400 µm solder balls were obtained through cutting, remelting, and selection processes. The printed circuit board was a custom-made FR-4 substrate with copper pads of 310 µm in diameter and 70 µm in thickness [27]. The surface of the printed circuit board was treated with an organic solder protectant. The solder balls were soldered to the copper pads on the FR-4 substrate after two soldering sessions using R340C reflow soldering. According to the melting point of Sn58Bi-xNi, the peak soldering temperature was set to 180 °C. The samples for indentation creep and hardness were polished to mirror-like and scratch-free after soldering. The sample preparation process of Cu/Sn58Bi-xNi/Cu micro solder joints is shown in Figure 1. The reflow temperature process curve is shown in Figure 2.

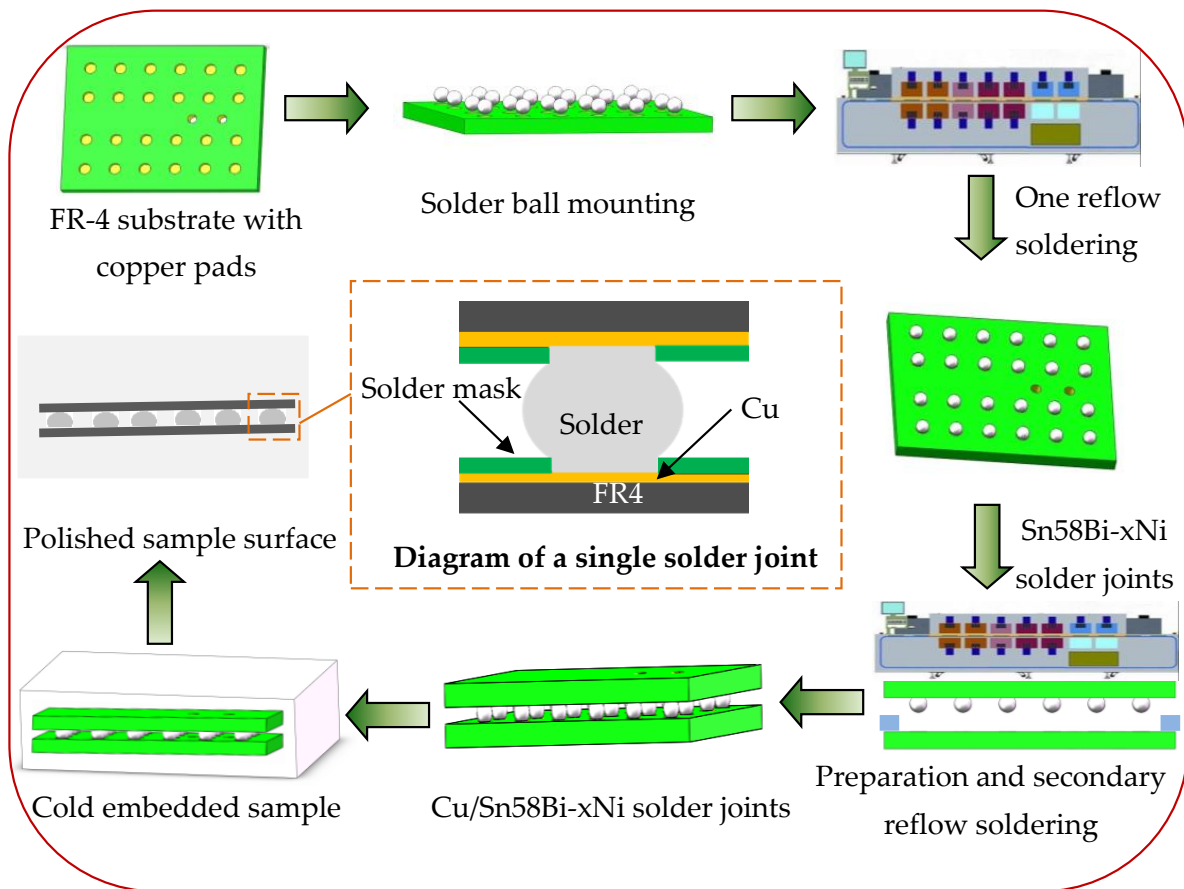


Figure 1. Schematic diagram of sample preparation process.

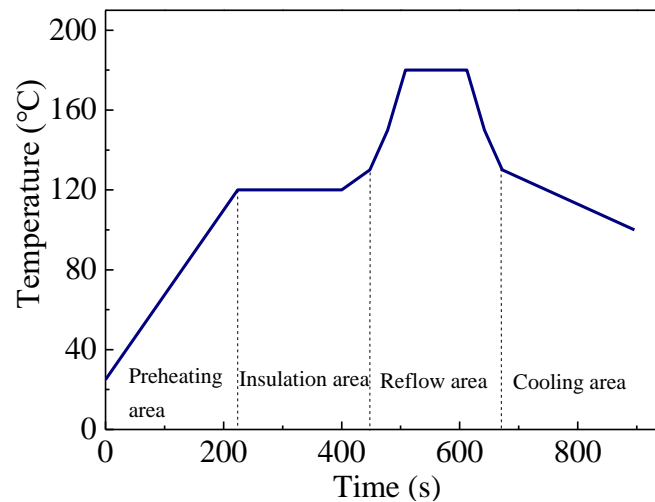


Figure 2. Reflow temperature process curve.

Creep is a slow, continuous, and irreversible deformation that occurs under constant temperature, load, and long-term action, often intensifying with increasing temperature. Hardness is the resistance to local deformation and one of the important indexes to evaluate the mechanical properties of materials. In the indentation test, the indentation hardness H_{IT} can be expressed by Formula (1) as [28]

$$H_{IT} = \frac{F_{\max}}{A_c} \quad (1)$$

where F_{\max} is the indentation testing maximum load, A_c is the projected area of indenter contact surface. For a 115° Berkovich-type indenter, A_c can be described as [28,29]

$$A_c = 24.56h_c^2 \quad (2)$$

where h_c is the depth of contact of the test specimen, and h_c can be represented as [28,29]

$$h_c = h_{\max} - \varepsilon(h_{\max} - h_r) \quad (3)$$

where ε is the shape correction factor of the indenter, which depends on the geometry of the indenter, and $\varepsilon = 0.75$; h_{\max} is the maximum indentation depth; h_r is the intersection of the tangent at the maximum load and the displacement axis during unloading.

The indentation creep and hardness of Cu/Sn58Bi-xNi/Cu micro solder joints under high temperatures were tested using a Shimadzu DUH-211S ultra-micro dynamic hardness tester, for which the indenter is a 115° Berkovich type. A self-designed micro heating device was installed on the indentation tester to realize the test at different temperatures. The schematic diagram of the micro heating table is shown in Figure 3. The test temperatures were 25°C , 50°C , 75°C , and 100°C , respectively. The Sn58Bi alloy has a stable microstructure at 80°C , but when the temperature exceeds 100°C , the Bi phase will grow abnormally, resulting in poor performance of the alloy [30]. Therefore, the test maximum temperature of the test was 100°C . The indentation testing maximum load was 20 mN, and the loading rate and unloading rate were both 5 mN/s. In order to obtain steady-state creep data, the holding time of the creep test was set to 600 s, continuing for 60 s at 90% of each test unloading to correct thermal drift. For this study, ν of Sn58Bi solder was considered to be 0.343 [31]. In each indentation process, the indentation space was larger than three times the indentation size in order to avert the adjacent indentation stress field influence [32]. Under each temperature test condition, more than ten independent indentations were tested. SEM was used to observe the microstructures of solder alloys and the indentation morphology

of micro solder joints at different temperatures. The flow chart of the experimental process is shown in Figure 4.

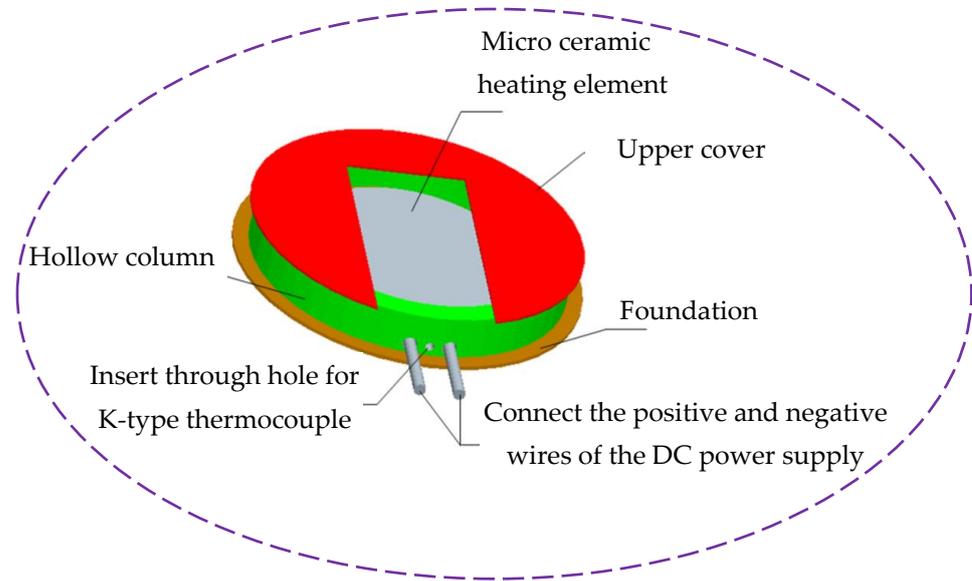


Figure 3. Schematic diagram of micro heating table.

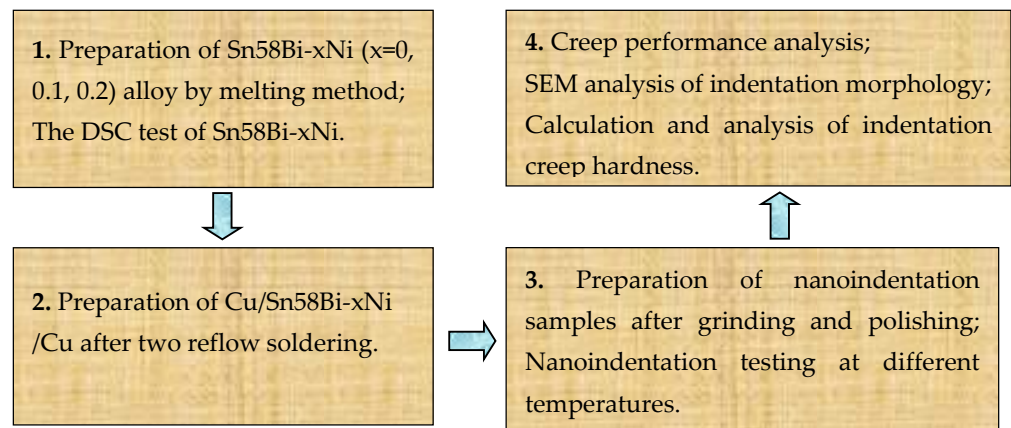


Figure 4. The flow chart of the experimental process.

3. Results and Discussion

3.1. Indentation Load–Depth Curves versus Different Temperatures

Figure 5 illustrates the indentation load versus depth curves of Cu/Sn58Bi-xNi/Cu micro solder joints at different temperatures. It can be seen that the indentation curves of Cu/Sn58Bi/Cu, Cu/Sn58Bi-0.1Ni/Cu, and Cu/Sn58Bi-0.2Ni/Cu micro solder joints move to the right during the loading stage. The initial indentation depth of Cu/Sn58Bi-0.1Ni/Cu micro solder joints at 25 °C, 50 °C, 75 °C, and 100 °C are $1.50 \pm 0.01 \mu\text{m}$, $1.59 \pm 0.02 \mu\text{m}$, $2.05 \pm 0.13 \mu\text{m}$, and $3.47 \pm 0.18 \mu\text{m}$, respectively. The results indicate that the initial indentation depth increases with the increase of temperature. In nanoindentation testing, the depth recorded at each load increment is usually the sum of the depths generated by the material's elastic–plastic and creep properties. During the holding stage, the platform length of the load–depth curve increases gradually, indicating that the creep depth increases with increasing temperature under the same load. In the unloading stage, the slope of the unloading curve is very large at test temperatures of 25 °C and 50 °C, and decreases at the high temperature, especially at 100 °C. The unloading curves of the load–depth

under different temperatures showed significant permanent deformation and insignificant elastic recovery for the three types of micro solder joints at 25 °C and 50 °C. However, elastic recovery was observed at 75 °C, and was more significant at 100 °C. The initial indentation depths of Cu/Sn58Bi/Cu, Cu/Sn58Bi-0.1Ni/Cu, and Cu/Sn58Bi-0.2Ni/Cu micro solder joints at 100 °C are $3.88 \pm 0.30 \mu\text{m}$, $3.47 \pm 0.18 \mu\text{m}$, and $3.83 \pm 0.26 \mu\text{m}$, respectively, and the slope of the indentation stage curve decreases, indicating that the micro solder joints undergo high softening. The minimum initial indentation depth of Cu/Sn58Bi-0.1Ni/Cu shows that it has the strongest resistance to high-temperature plastic deformation. In addition, the indentation depths of Cu/Sn58Bi/Cu, Cu/Sn58Bi-0.1Ni/Cu, and Cu/Sn58Bi-0.2Ni/Cu micro solder joints increase from $3.02 \pm 0.03 \mu\text{m}$, $2.33 \pm 0.02 \mu\text{m}$, and $2.86 \pm 0.02 \mu\text{m}$ at 25 °C to $7.45 \pm 0.42 \mu\text{m}$, $6.22 \pm 0.28 \mu\text{m}$, and $6.36 \pm 0.25 \mu\text{m}$ at 100 °C, respectively. Among them, the indentation depth of Cu/Sn58Bi/Cu micro solder joints varies the most with temperature. Addition of an appropriate amount of Ni element to Cu/Sn58Bi/Cu micro solder joints can prevent the increase of indentation depth under the same indentation load.

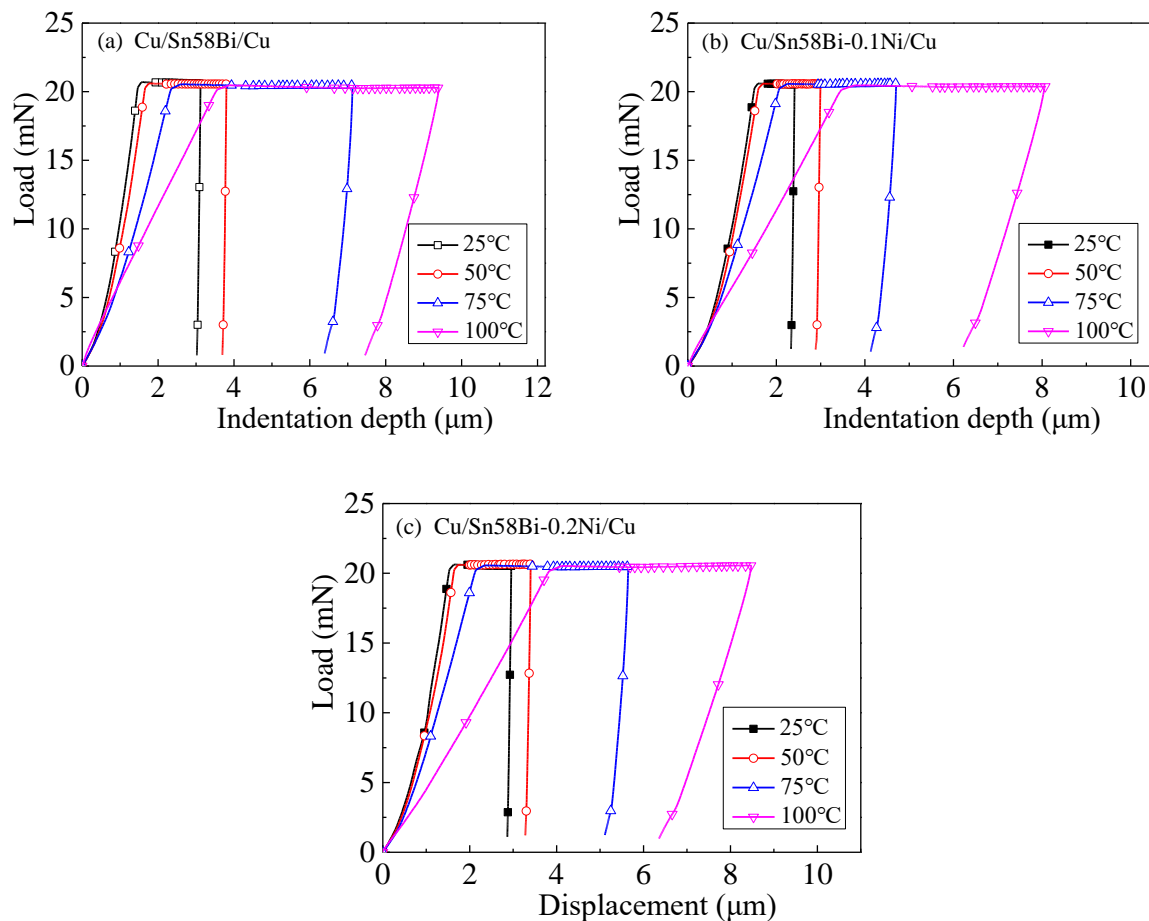


Figure 5. Indentation load–depth curves of micro solder joints at different temperatures (a) Cu/Sn58Bi/Cu, (b) Cu/Sn58Bi-0.1Ni/Cu, and (c) Cu/Sn58Bi-0.2Ni/Cu.

3.2. Creep Displacement with Different Temperatures

In the process of creep, creep displacement is also one of the useful metrics to comprehensively assess the creep behavior of a material [33]. Under each temperature test, a constant loading rate was adopted and then the constant loading was maintained for 600 s to study the creep deformation as a function of time. A curve of the creep displacement against holding time was obtained under different temperatures, as shown in Figure 6. At the beginning of creep, creep displacement increases rapidly. With the increase of creep

time, creep displacement increases slowly and enters the steady-state creep stage. The creep displacement values of Cu/Sn58Bi/Cu, Cu/Sn58Bi-0.1Ni/Cu, and Cu/Sn58Bi-0.2Ni/Cu micro solder joints are $4.39 \pm 0.30 \mu\text{m}$, $2.36 \pm 0.24 \mu\text{m}$, and $3.11 \pm 0.26 \mu\text{m}$ at 75°C , respectively. By comparison, the addition of Ni elements in the micro solder joints exhibits smaller creep displacement at high temperatures and a better creep resistance. Research has shown that Ni can refine the microstructure in the solder alloy, and Ni_3Sn_4 IMC particles formed in the alloy; therefore, it can increase the resistance to dislocation, which improves the creep properties [34–36]. In addition, it can be seen from Figure 6 that the creep displacement increases with the increase of temperature. This is because in the high temperature indentation stress field, the diffusion and movement of atoms or the movement of dislocations are enhanced, resulting in a decrease in grain boundary strength. The microstructures of Sn58Bi-xNi solder alloys with different mass fractions of Ni elements by SEM are shown in Figure 7. The gray bright zone is the mainly Bi-rich phase, and the darkly pigmented zone is the mainly Sn-rich phase. From Figure 7, it can be seen that the addition of Ni element reduces the number of Bi-rich dendrites, plays a role in refining the grains, and is manifested as an increase in the number of grain boundaries per unit area. Furthermore, due to the addition of Ni elements, Ni reacts with Sn to form compounds, and more grain boundaries exist in the soldering alloy [21], which can improve the creep resistance of Cu/Sn58Bi/Cu micro solder joints at high temperatures. Creep continues to occur with the passage of time and the increase of temperature, leading to a decrease in the ability of micro solder joints to resist creep deformation at high temperatures.

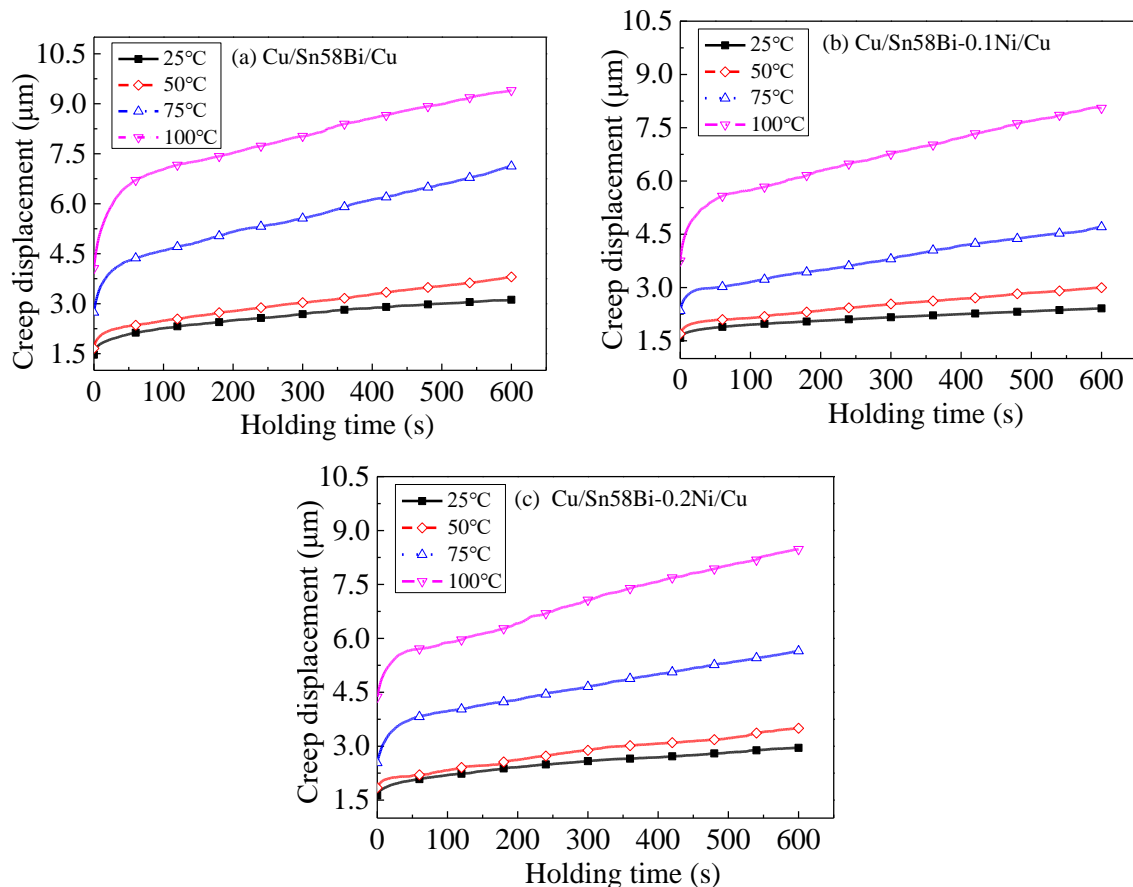


Figure 6. Holding time–creep displacement curves of micro solder joints at different temperatures (a) Cu/Sn58Bi/Cu, (b) Cu/Sn58Bi-0.1Ni/Cu, and (c) Cu/Sn58Bi-0.2Ni/Cu.

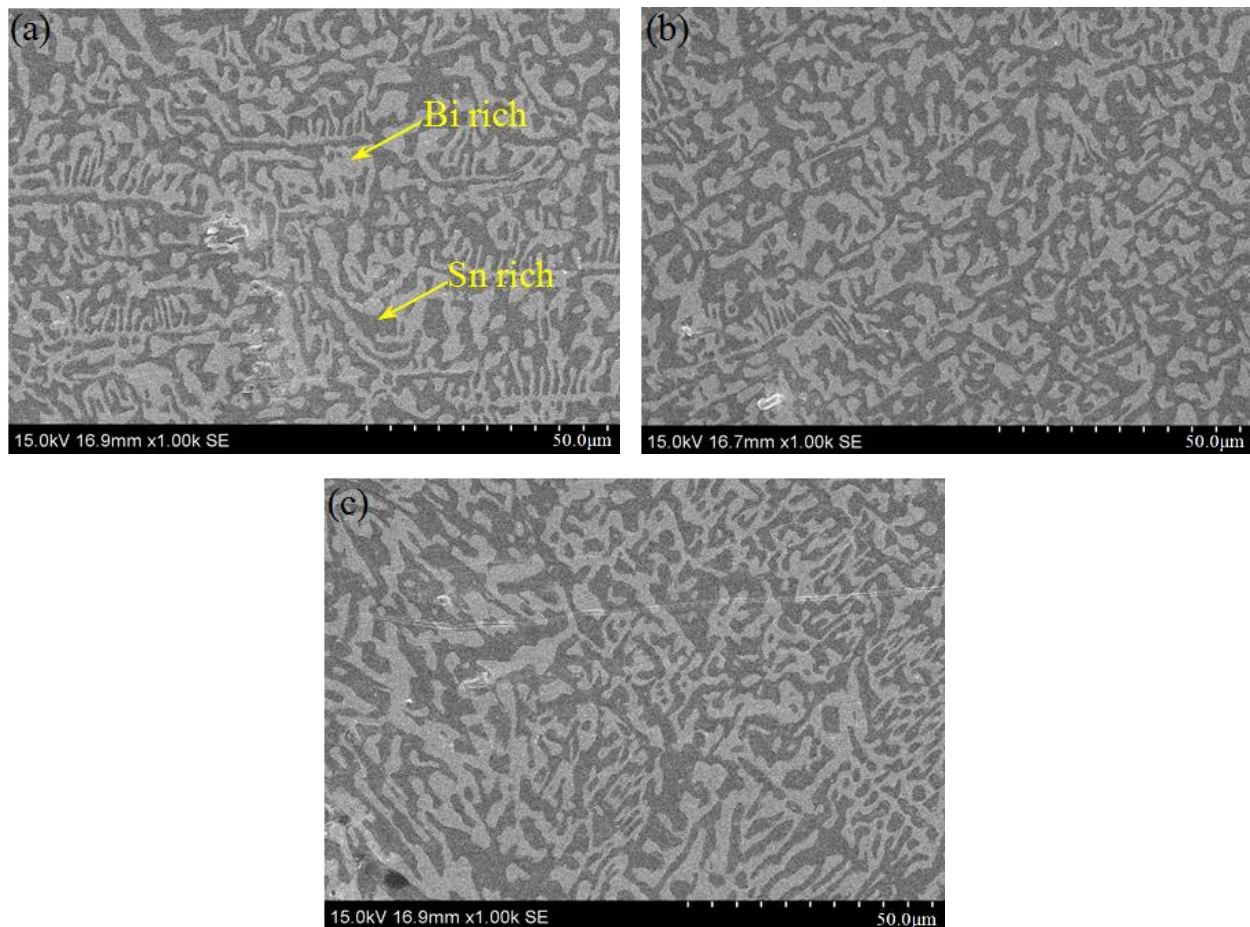


Figure 7. Microstructures of solder alloys (a) Sn58Bi, (b) Sn58Bi-0.1Ni, and (c) Sn58Bi-0.2Ni.

3.3. Influence of Temperature on Indentation Morphology

In nanoindentation testing, the indentation morphology can reflect the plastic deformation of solder alloy [37]. The indentation morphologies of Cu/Sn58Bi/Cu, Cu/Sn58Bi-0.1Ni/Cu, and Cu/Sn58Bi-0.2Ni/Cu micro solder joints at different temperatures are presented in Figures 8–10. From Figures 8–10, it can be clearly seen that the indentation size of the three types of micro solder joints increases continuously with the increase of temperature. The higher the temperature, the greater the energy provided by thermal activation, and the more vacancies generated, making the movement of dislocations easier. Solder is more prone to produce creep deformation during the load-holding stage. Therefore, the increase in temperature gradually increases the degree of creep deformation of the solder, manifested as the size of the indentation increasing with the increase of temperature. In addition, at higher temperatures, the solder softens, and the stress below the indenter is released in a plastic deformation manner in a short period of time, resulting in an increase in the size of the indentation. This result is similar to the research of Fan et al. [32]. Under the same temperature conditions, Ni doping can reduce the indentation area. The indentation size of Cu/Sn58Bi-0.1Ni/Cu is the smallest among the three types of micro solder joints, and its high-temperature creep resistance is the best.

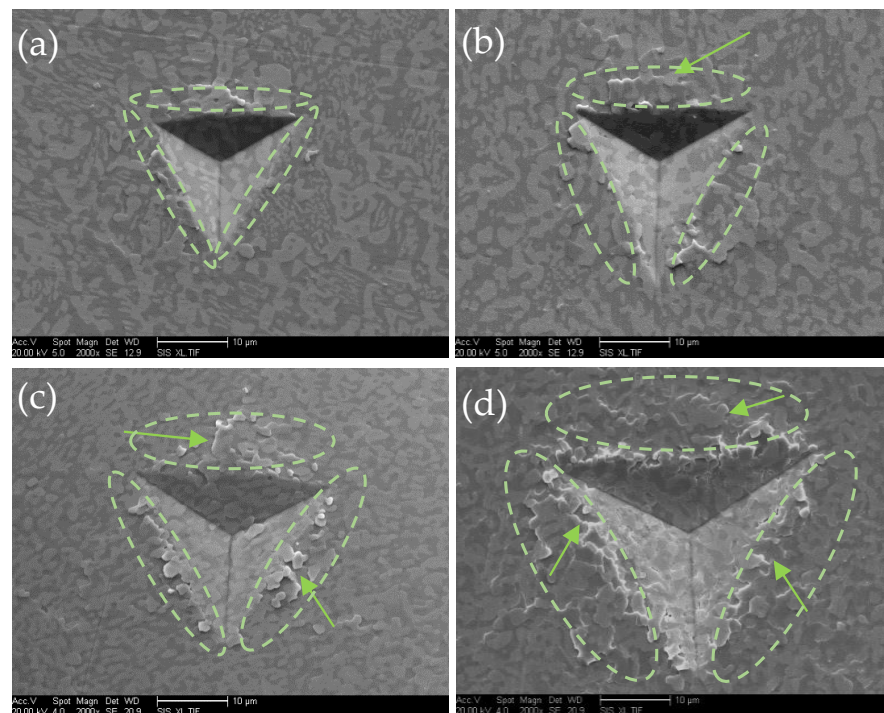


Figure 8. SEM image of indentations made on Cu/Sn58Bi/Cu micro solder joints at different temperatures (arrows indicate accumulation around the indentation): (a) 25 °C, (b) 50 °C, (c) 75 °C, and (d) 100 °C.

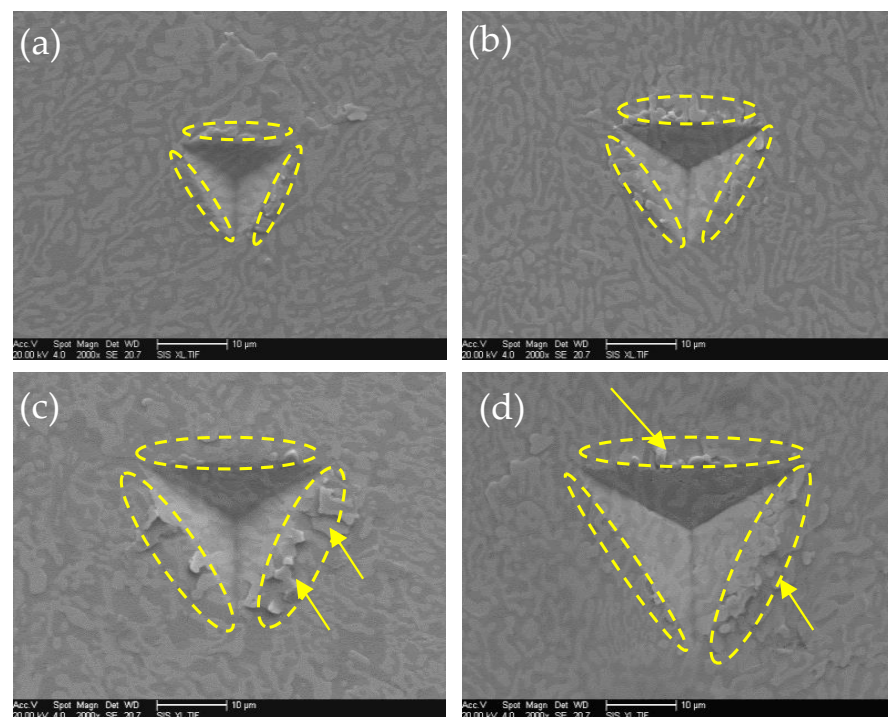


Figure 9. SEM image of indentations made on Cu/Sn58Bi-0.1Ni/Cu micro solder joints at different temperatures (arrows indicate accumulation around the indentation): (a) 25 °C, (b) 50 °C, (c) 75 °C, and (d) 100 °C.

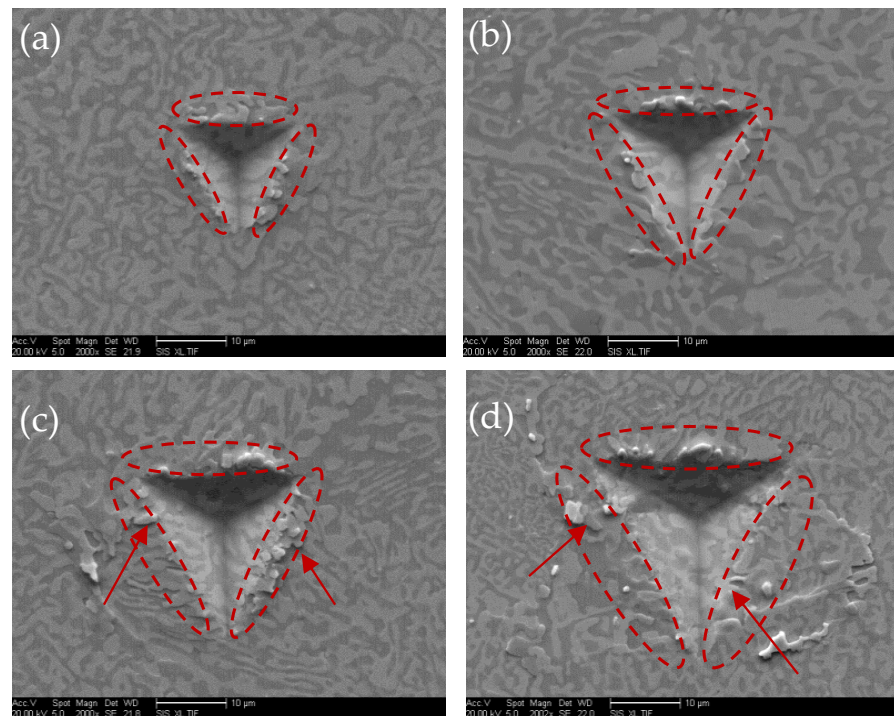


Figure 10. SEM image of indentations made on Cu/Sn58Bi-0.2Ni/Cu micro solder joints at different temperatures (arrows indicate accumulation around the indentation): (a) 25 °C, (b) 50 °C, (c) 75 °C, and (d) 100 °C.

It can be observed from Figures 8–10 that there is an accumulation phenomenon around the indentations (arrows indicate accumulation around the indentation, circles represent the area of influence around the indentation), mainly caused by the plastic flow of the solder. For some materials, especially some low-strain-hardening solder, a large number of dislocations are generated near the indenter during the indentation test [32]. Due to the movement of dislocations, plastic deformation occurs in the solder below the indenter. Through the movement of the indenter, part of the solder is pushed out to the side of the indenter and forms accumulation phenomenon, which makes the projected contact area larger than the cross-sectional area of the indenter [38]. Especially at 75 °C and 100 °C, as the temperature increases, the size of the indentation gradually increases, and the accumulation degree and influence area around the indentation gradually increase. Li and Warren [39] proposed that the highly concentrated indentation stress field in the sample material leads to a chemical potential gradient, resulting in thermally activated atomic diffusion flux flowing from the region below the indentation to the sample surface and along the interface between the indentation and the sample. The higher the temperature, the larger the thermally activated atomic diffusion flux, and the more obvious the accumulation phenomenon on the indentation surface. Under the same experimental conditions, combining Figures 8–10, Ni doping can reduce the indentation area and accumulation phenomenon around the indentation.

The microstructure, after adding different Ni contents, can also be observed from Figures 8–10. In Figure 8, Sn58Bi is composed of an eutectic structure, where the dark phase and bright phase are Sn- and Bi-rich phases, respectively. After adding Ni to Sn58Bi solder, Ni reacts with Sn to form Ni-Sn intermetallic compound in the solder [21,25,34]. When the addition of Ni is 0.1 wt.%, Ni can provide more nucleation particles for the Sn-rich phase precipitated first, forming intermetallic compound Ni_3Sn_4 , and refining the microstructure. The presence of a moderate amount of Ni_3Sn_4 in solder joints can also improve the creep resistance at high temperatures. When the addition of Ni is 0.2 wt.%, the fine granular new products in the microstructure of the solder begin to aggregate and

grow, while the aggregated Ni_3Sn_4 cannot effectively inhibit grain growth, resulting in a coarser microstructure of the solder and reduced high-temperature creep resistance. This result is consistent with the research of Shen et al. [40], whereby the creep resistance of Sn58Bi composite solder first increases and then decreases with the increase of Ni content, confirming that Ni could improve the microstructure of Sn58Bi solder, which results in the creep resistance being reinforced.

3.4. Indentation Hardness at Different Temperatures

According to the indentation load–depth curves in Figure 5 and Formulas (1)–(3), the H_{IT} values of Cu/Sn58Bi/Cu, Cu/Sn58Bi-0.1Ni/Cu, and Cu/Sn58Bi-0.2Ni/Cu micro solder joints were obtained at different temperatures. The variation of indentation creep hardness with temperature for the three types of micro solder joints is shown in Figure 11. As can be seen from Figure 11, the addition of a small amount of Ni elements can appropriately improve the indentation hardness of Cu/Sn58Bi/Cu micro solder joints. This is consistent with the research results of Yang et al. [22] and Shen et al. [40]. Yang et al. [22] used a nanoindentation method to test the hardness of Sn58Bi, Sn58Bi-0.5Ni, and Sn58Bi-1Ni solder alloys. The results show that the hardness of solder alloys increases with the increase of Ni content and decreases with the extension of aging time. Shen et al. [40] investigated the effect of nano-Ni particles on the hardness of 42% Sn-58%Bi using the indentation method. The results indicate that the hardness of 42% Sn-58%Bi alloy steadily increases with the increase of nano-Ni concentration. The hardening effect of metal alloys not only comes from the hard IMC phase, but also from the strengthening of the matrix alloy due to the refinement of the microstructure. Due to differences in experimental conditions, equipment, the state of the solder alloys, and the state and content of the reinforcing phase, the measured hardness values may vary. However, the research findings are similar, indicating that the addition of Ni can improve the hardness of Sn58Bi solder alloy. Nevertheless, the indentation hardness is correlated with temperature. The indentation hardness of three types of micro solder joints decreases with the increase of temperature. The indentation hardness values of micro solder joints of Cu/Sn58Bi/Cu, Cu/Sn58Bi-0.1Ni/Cu, and Cu/Sn58Bi-0.2Ni/Cu at 100 °C are 14.67 ± 2.00 MPa, 21.05 ± 2.00 MPa, and 20.13 ± 2.10 MPa, respectively. This was mainly due to the ions in the micro solder joints absorbing heat energy during the heating process and reaching a larger amplitude equilibrium state, the higher temperature leads to softening of the micro solder joints, increasing the indentation depth and reducing the indentation hardness [41].

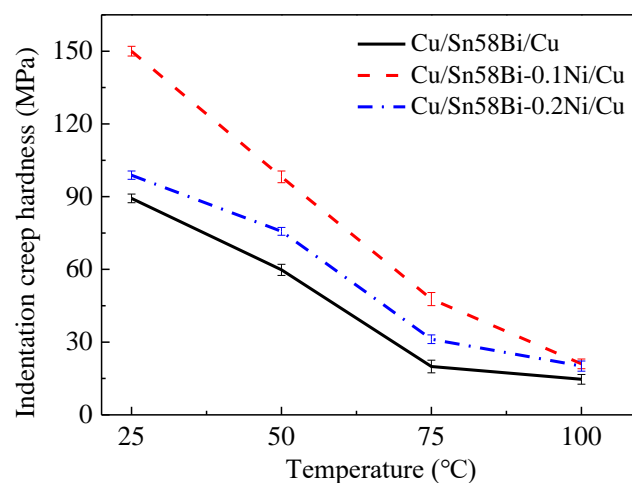


Figure 11. The H_{IT} of Cu/Sn58Bi/Cu, Cu/Sn58Bi-0.1Ni/Cu, and Cu/Sn58Bi-0.2Ni/Cu micro solder joints at different temperatures.

In addition, the melting points of the three types of solders tested by DSC are 139.90 °C, 140.18 °C, and 139.27 °C, respectively, as shown in Figure 12. According to the comparison temperature T (the ratio of working temperature to melting point temperature T_{melt}), a good indicator of dislocation migration rate is provided. The evaluation of material creep characteristics usually involves four key parameters: loading stress, experimental temperature, creep rate in the steady-state stage, and failure time. When the comparison temperature is within the temperature range of $0.3 T_{\text{melt}} < T < 0.9 T_{\text{melt}}$, it belongs to the creep caused by dislocation migration [42]. Under experimental conditions of 100 °C, the calculated comparative temperatures T of the three type solders are 0.715, 0.713, and 0.718, respectively, resulting in creep deformation caused by dislocation migration. Creep deformation at high temperatures is also an important reason for the decrease in mechanical properties of materials.

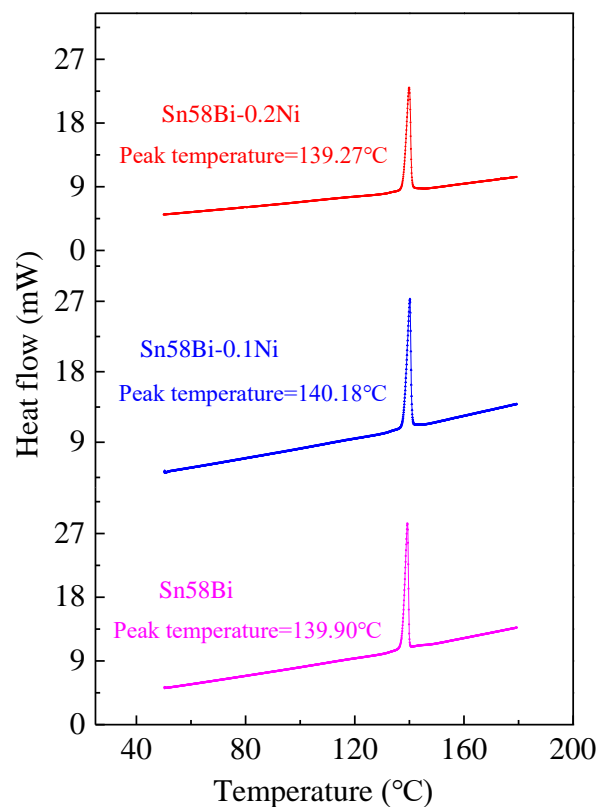


Figure 12. DSC test curves of Sn58Bi, Sn58Bi-0.1Ni, and Sn58Bi-0.2Ni solder.

4. Conclusions

In this work, the influence of Ni addition on indentation creep and hardness of Cu/Sn58Bi-xNi/Cu micro solder joints at high temperatures has been investigated. The following conclusions can be drawn:

- (1) Under the same experimental conditions, the initial indentation depth and creep displacement of Cu/Sn58Bi/Cu micro solder joints can be reduced by adding a small amount of Ni elements. The creep displacement values of Cu/Sn58Bi/Cu, Cu/Sn58Bi-0.1Ni/Cu, and Cu/Sn58Bi-0.2Ni/Cu micro solder joints at 75 °C were $4.39 \pm 0.30 \mu\text{m}$, $2.36 \pm 0.24 \mu\text{m}$ and $3.11 \pm 0.26 \mu\text{m}$, respectively. Among the three types of micro solder joints, Cu/Sn58Bi-0.1Ni/Cu exhibited the best creep resistance at high temperatures.
- (2) According to the observation of the indentation morphology at different temperatures, it was found that there was accumulation around the indentation, especially at 75 °C and 100 °C. Compared with Cu/Sn58Bi/Cu micro solder joints, Cu/Sn58Bi-0.1Ni/Cu and Cu/Sn58Bi-0.2Ni/Cu had smaller indentation areas and less accu-

mulation around the indentation. Ni doping can reduce the indentation area and accumulation phenomenon around the indentation.

- (3) The indentation hardness values of micro solder joints of Cu/Sn58Bi/Cu, Cu/Sn58Bi-0.1Ni/Cu, and Cu/Sn58Bi-0.2Ni/Cu at 100 °C were 14.67 ± 2.00 MPa, 21.05 ± 2.00 MPa, and 20.13 ± 2.10 MPa, respectively. Due to the melting points of the three types of solder alloys, which were 139.90 °C, 140.18 °C, and 139.27 °C, respectively, the solder softened during indentation testing at 100 °C, resulting in a sharp decrease in creep hardness.

Author Contributions: Conceptualization, methodology, writing—original draft, and funding acquisition, X.K.; investigation, methodology, and funding acquisition, J.Z.; investigation, data curation, and visualization, R.M.; methodology, writing—review editing, and formal analysis, F.S. and X.L. All authors have read and agreed to the published version of the manuscript.

Funding: This research was funded by the National Natural Science Foundation of China (No. 12002003), Natural Science Foundation of Hebei Province (No. E2021409021 and A2023409007), Science and Technology Research Foundation for Universities of Hebei Province (No. ZD2020131 and QN2023042), Langfang Youth Talent Support Program (No. LFBJ202001 and LFBJ202204), and “333 Project” of Hebei Province (No. C20221033).

Institutional Review Board Statement: Not applicable.

Informed Consent Statement: Not applicable.

Data Availability Statement: The original contributions presented in the study are included in the article, further inquiries can be directed to the corresponding authors.

Conflicts of Interest: The authors declare no conflicts of interest.

References

1. Tian, Y.N.; Jian, X.D.; Zhao, M.R.; Liu, J.H.; Dai, X.J.; Zhou, B.; Yang, X.F. Effect of thermal aging on the reliability of interconnected nano-silver solder joints. *Crystals* **2023**, *13*, 1630. [\[CrossRef\]](#)
2. Song, Q.Q.; Yang, W.C.; Li, Y.T.; Mao, J.; Qin, W.O.; Zhan, Y.Z. Interfacial reaction and mechanical properties of Sn58Bi-XCr solder joints under isothermal aging conditions. *Vacuum* **2021**, *194*, 110559. [\[CrossRef\]](#)
3. Gao, Y.; Zhang, K.; Zhang, C.; Wang, Y.; Chen, W. Microstructure and properties of electromigration of Sn58Bi/Cu solder joints with different joule thermal properties. *Metals* **2023**, *13*, 1475. [\[CrossRef\]](#)
4. Dušek, K.; Buek, D.; Vesel, P.; Anna, P.; Plaek, M.; Re, J.D. Understanding the effect of reflow profile on the metallurgical properties of tin-bismuth solders. *Metals* **2022**, *12*, 121. [\[CrossRef\]](#)
5. Singh, A.; Durairaj, R. Study on hardness and shear strength with microstructure properties of Sn52Bi/Cu+1% Al₂O₃ nanoparticles. In Proceedings of the IOP Conference Series: Materials Science and Engineering, Chennai, India, 16–17 September 2020; Volume 834, pp. 1–5.
6. Liu, Y.; Chang, J.; Zhou, M.; Xue, Y.; Sun, F. Microstructure and shear behavior of Sn58Bi/Cu solder joint enhanced by SnAgCuBiNi bump. *Mod. Phys. Lett. B* **2020**, *34*, 2050413. [\[CrossRef\]](#)
7. Hirata, Y.; Yang, C.H.; Lin, S.; Nishikawa, H. Improvements in mechanical properties of Sn-Bi alloys with addition of Zn and In. *Mat. Sci. Eng. A-Struct.* **2021**, *813*, 141131. [\[CrossRef\]](#)
8. Kang, H.; Rajendran, S.H.; Jung, J.P. Low melting temperature Sn-Bi solder: Effect of alloying and nanoparticle addition on the microstructural, thermal, interfacial bonding, and mechanical characteristics. *Metals* **2021**, *11*, 364. [\[CrossRef\]](#)
9. Shen, Y.A.; Zhou, S.; Li, J.; Tu, K.N.; Nishikawa, H. Thermomigration induced microstructure and property changes in Sn-58Bi solders. *Mater. Des.* **2019**, *166*, 107619. [\[CrossRef\]](#)
10. Han, J.; Cao, H.; Meng, Z.; Jin, X.L.; Ma, L.M.; Guo, F.; An, T.; Wang, T. Study on electromigration mechanism of lead-free Sn3.5Ag0.5Bi8.0In solder joints. *J. Electron. Mater.* **2023**, *52*, 1216–1232. [\[CrossRef\]](#)
11. Wang, X.; Zhang, L.; Chen, C.; Lu, X. Effect of AlN on the microstructure evolution of Cu/Sn58Bi/Cu solder joints for 3D packaging at different bonding times. *J. Mater. Res. Technol.* **2023**, *25*, 4488–4496. [\[CrossRef\]](#)
12. Yang, L.; Ma, S.; Mu, G. Improvements of microstructure and hardness of lead-free solders doped with Mo nanoparticles. *Mater. Lett.* **2021**, *304*, 130654. [\[CrossRef\]](#)
13. Singh, A.; Durairaj, R.; Kumar, K.G.; Kuan, S.H. Impact of 3% Molybdenum(Mo) nanoparticles on the interfacial and shear properties of lead-free Sn58Bi/Cu solder joint. In Proceedings of the IOP Conference Series: Materials Science and Engineering, Chandigarh, India, 4–5 March 2022; p. 012029.
14. Li, Y.; Yu, S.; Li, L.; Song, S.; Qin, W.; Qi, D.; Yang, W.; Zhan, Y. A review on the development of adding grapheneto Sn-based lead-free solder. *Metals* **2023**, *13*, 1209. [\[CrossRef\]](#)

15. Huang, X.; Zhang, L.; Chen, C.; Lu, X.; Wang, X. Comprehensive analysis of Sn58Bi/Cu solder joints reinforced with Mg particles: Wettability, thermal, mechanics, and microstructural characterization. *J. Mater. Res. Technol.* **2023**, *27*, 2641–2655. [[CrossRef](#)]
16. Jeong, G.; Yu, D.Y.; Baek, S.; Bang, J.H.; Ko, Y.H. Interfacial reactions and mechanical properties of Sn-58Bi solder joints with Ag nanoparticles prepared using ultra-fast laser bonding. *Materials* **2021**, *14*, 335. [[CrossRef](#)]
17. Yang, F.; Zhang, L.; Liu, Z.Q.; Zhong, S.; Ma, J.; Bao, L. Effects of CuZnAl particles on properties and microstructure of Sn-58Bi solder. *Materials* **2017**, *10*, 558. [[CrossRef](#)] [[PubMed](#)]
18. Qin, W.; Yang, W.; Zhang, L.; Qi, D.; Song, Q.; Zhan, Y. Effect of Ni-modified reduced graphene oxide on the mechanical properties of Sn-58Bi solder joints. *Vacuum* **2023**, *211*, 111943. [[CrossRef](#)]
19. Nogita, K.; Nishimura, T. Nickel-stabilized hexagonal (Cu, Ni)₆Sn₅ in Sn-Cu-Ni lead free solder alloys. *Scripta Mater.* **2008**, *59*, 191–194. [[CrossRef](#)]
20. Nogita, K.; McDonald, S.D.; Tsukamoto, H.; Read, J.; Nishimura, T. Inhibiting cracking of interfacial Cu₆Sn₅ by Ni additions to Sn-based lead-free solders. *Trans. Jpn. Inst. Electron. Packag.* **2009**, *2*, 46–54. [[CrossRef](#)]
21. Kanlayasiri, K.; Ariga, T. Physical properties of Sn58Bi-xNi lead-free solder and its interfacial reaction with copper substrate. *Mater. Des.* **2015**, *86*, 371–378. [[CrossRef](#)]
22. Yang, L.Z.; Zhou, W.; Ma, Y.; Li, X.Z.; Liang, Y.H.; Cui, W.Q.; Wu, P. Effects of Ni addition on mechanical properties of Sn58Bi solder alloy during solid-state aging. *Mat. Sci. Eng. A* **2016**, *667*, 368–375. [[CrossRef](#)]
23. Fleshman, C.; Duh, J.G. The variation of microstructure and the improvement of shear strength in SAC1205-xNi/OSP Cu solder joints before and after aging. *J. Electron. Mater.* **2020**, *49*, 196–201. [[CrossRef](#)]
24. Cao, C.C.; Zhang, K.K.; Shi, B.J.; Wang, H.G.; Zhao, D.; Sun, M.M.; Zhang, C. The interface microstructure and shear strength of Sn_{2.5}Ag_{0.7}Cu_{0.1}RExNi/Cu solder joints under thermal-cycle loading. *Metals* **2019**, *9*, 518. [[CrossRef](#)]
25. Yang, L.Z.; Zhou, W.; Li, X.Z.; Ma, Y.; Liang, Y.H.; Cui, W.Q.; Wu, P. Effect of Ni and Ni-coated Carbon Nanotubes on the interfacial reaction and growth behavior of Sn58Bi/Cu intermetallic compound layers. *J. Mater. Sci. Mater. Electron.* **2016**, *27*, 12264–12270. [[CrossRef](#)]
26. Wang, H.Z.; Hu, X.W.; Jiang, X.G. Effects of Ni modified MWCNTs on the microstructural evolution and shear strength of Sn-3.0Ag-0.5Cu composite solder joints. *Mater. Charact.* **2020**, *163*, 110287. [[CrossRef](#)]
27. Zhang, H.W.; Liu, Y.; Wang, J.; Sun, F.L. Failure study of solder joints subjected to random vibration loading at different temperatures. *J. Mater. Sci.-Mater. Electron.* **2015**, *26*, 2374–2379. [[CrossRef](#)]
28. Khodabakhshi, F.; Zareghomsheh, M.; Khatibi, G. Nanoindentation creep properties of lead-free nanocomposite solders reinforced by modified carbon nanotubes. *Mat. Sci. Eng. A* **2020**, *797*, 140203. [[CrossRef](#)]
29. Cordova, M.E.; Shen, Y.L. Indentation versus uniaxial power-law creep: A numerical assessment. *J. Mater. Sci.* **2015**, *50*, 1394–1400. [[CrossRef](#)]
30. Qun, L.I.; Huang, J.H.; Zhang, H.; Zhao, X.K.; Qi, L.H. Influence of Al on microstructure and mechanical properties of the Sn-58Bi lead-free solder. *Electron. Process Technol.* **2008**, *29*, 3471–3474.
31. Yang, L.Z.; Zhou, W.; Liang, Y.H.; Cui, W.Q.; Wu, P. Improved microstructure and mechanical properties for Sn58Bi solder alloy by addition of Ni-coated carbon nanotubes. *Mater. Sci. Eng. A* **2015**, *642*, 7–15. [[CrossRef](#)]
32. Fan, J.J.; Jiang, D.W.; Zhang, H.; Hu, D.; Liu, X.; Fan, X.J.; Zhang, G.Q. High-temperature nanoindentation characterization of sintered nano-copper particles used in high power electronics packaging. *Results Phys.* **2022**, *33*, 105168. [[CrossRef](#)]
33. Thornby, J.; Harris, A.; Bird, A.; Beake, B.; Haghsheenas, M. Micromechanics and Indentation Creep of Magnesium Carbon Nanotube Nanocomposites: 298 K–573 K. *Mater. Sci. Eng. A* **2021**, *801*, 140418. [[CrossRef](#)]
34. El-Daly, A.A.; Hammad, A.E.; Fawzy, A.; Nasrallah, D.A. Microstructure, mechanical properties, and deformation behavior of Sn-1.0Ag-0.5Cu solder after Ni and Sb additions. *Mater. Des.* **2013**, *43*, 40–49. [[CrossRef](#)]
35. Che, F.X.; Zhu, W.H.; Poh, E.S.W.; Zhang, X.R.; Zhang, X.W.; Chai, T.C.; Gao, S. Creep properties of Sn-1.0Ag-0.5Cu lead-free solder with Ni addition. *J. Electron. Mater.* **2011**, *40*, 344–354. [[CrossRef](#)]
36. Silva, B.L.; Cheung, N.; Garcia, A.; Spinelli, J.E. Sn-0.7wt%Cu-(xNi) alloys: Microstructure-mechanical properties. correlations with solder/substrate interfacial heat transfer coefficient. *J. Alloys Compd.* **2015**, *632*, 274–285. [[CrossRef](#)]
37. Han, Y.D.; Gao, Y.; Zhang, S.T.; Jing, H.Y.; Xu, L.Y. Study of mechanical properties of Ag nanoparticle-modified graphene/Sn-Ag-Cu solders by nanoindentation. *Mater. Sci. Eng.* **2019**, *761*, 138051.1–138051.13. [[CrossRef](#)]
38. Fischer-Cripps, A.C. *Nanoindentation Testing*; Springer: New York, NY, USA, 2011; pp. 89–90.
39. Li, W.B.; Warren, R. A model for nano-indentation creep. *Acta Metall. Mater.* **1993**, *41*, 3065–3069. [[CrossRef](#)]
40. Shen, L.; Tan, Z.Y.; Chen, Z. Nanoindentation study on the creep resistance of SnBi solder alloy with reactive nano-metallic fillers. *Mater. Sci. Eng. A* **2013**, *561*, 232–238. [[CrossRef](#)]
41. Sun, Y.; Liang, J.; Xu, Z.H.; Wang, G.F.; Li, X.D. Nanoindentation for measuring individual phase mechanical properties of lead free solder alloy. *J. Mater. Sci.-Mater. Electron.* **2008**, *19*, 514–521. [[CrossRef](#)]
42. Geng, D.C.; Yu, H.; Okuno, Y.; Kondo, S.; Kasada, R. Practical method to determine the effective zero-point of indentation depth for continuous stiffness measurement nanoindentation test with Berkovich tip. *Sci. Rep.* **2022**, *12*, 6391. [[CrossRef](#)]

Disclaimer/Publisher’s Note: The statements, opinions and data contained in all publications are solely those of the individual author(s) and contributor(s) and not of MDPI and/or the editor(s). MDPI and/or the editor(s) disclaim responsibility for any injury to people or property resulting from any ideas, methods, instructions or products referred to in the content.